Biosensors and Bioelectronics 53 (2014) 479–485

Contents lists available at ScienceDirect

Biosensors and Bioelectronics

journal homepage: www.elsevier.com/locate/bios

The unfolding of G-quadruplexes and its adverse effect on DNA—gold nanoparticles-based sensing system

Sheng Cheng [a,b], Bin Zheng [a,b], Mozhen Wang [a,*], Xuewu Ge [a,*], Qing Zhao [b], Wei Liu [a,b], Michael Hon-Wah Lam [b]

[a] CAS Key Laboratory of Soft Matter Chemistry, Department of Polymer Science and Engineering, University of Science and Technology of China and USTC-CityU Joint Advanced Research Center, Suzhou, PR China
[b] Department of Biology and Chemistry, City University of Hong Kong and USTC-CityU Joint Advanced Research Center, Suzhou, PR China

ARTICLE INFO

Article history:
Received 17 August 2013
Received in revised form
2 October 2013
Accepted 10 October 2013
Available online 24 October 2013

Keywords:
G-quadruplex
Unfolding
Gold nanoparticle
Biosensor
Lead ion

ABSTRACT

The adsorption of DNAs in G-quadruplex solution onto 13 nm gold nanoparticles (AuNPs) was studied through monitoring of the localized surface plasmon resonance (LSPR) absorbance of 13 nm AuNPs at 520 and 650 nm (A_{650}/A_{520}) in the solutions of three widely studied guanine-rich sequences, TBA (5′-GGTTGGTGTGGTTGG-3′), PW17(5′-GGGTAGGGCGGGTTGGG-3′), and PSO (5′-GGGTTAGGGTTAGGGT-TAGGG-3′). It was found that the degree of adsorption of DNAs in Pb^{2+} stabilized G-quadruplex (G-Pb^{2+}) solutions is up to 93% after more than 5 h of incubation. Furthermore, the lead concentrations in the solutions containing G-quadruplex and AuNP were analyzed by an inductively coupled plasma atomic emission spectrometer. The results showed that Pb^{2+} had been released from the G-quadruplexes, which means the G-quadruplexes may be unfolded in the presence of AuNP. This interaction between G-quadruplexes and AuNP demonstrated that long time incubation between DNAs and AuNPs would possibly make it unable to distinguish G-quadruplex from ssDNA. Thus, a biosensing system consisting of PW17 and AuNPs was developed to detect Pb^{2+}. It was found that the LSPR responses at A_{650}/A_{520} were sensitive to [Pb^{2+}]. However, the sensitivity of the system was interfered by the potential unfolding of PW17-Pb^{2+} in the presence of AuNPs. This unexpected adverse effect of AuNPs on DNA-based biosensors should be taken into consideration in the future development of biosensing systems that are based on ssDNA aptamers and unmodified AuNPs.

1. Introduction

In recent years, biosensors using aptamers or DNAzymes/RNAzymes as recognition units have attracted intense interest. Aptamers are single-stranded DNAs (ssDNA) or RNAs that have high affinity to a specific target molecule (Breaker, 1997; Ellington and Szostak, 1990), while DNAzymes/RNAzymes are nucleic acids that can catalyze a broad range of reactions (Wei et al., 2008). Because of the convenience in their synthesis, storage and modification (Jayasena, 1999; Zhang et al., 2011), aptamers have been used as the recognition units for the biosensing of a wide range of analytes, such as cocaine (Zhang et al., 2008), ATP (Wang et al., 2007), theophylline (Chavez et al., 2010), Ochratoxin A (Yang et al., 2011), potassium ions (Ueyama et al., 2002; Wang et al., 2006), mercury ions (Lee et al., 2007), and lead ions (Li et al., 2010a,b; Liu and Lu, 2003; Wei et al., 2008). With the incorporation of suitable chromophores or luminophores, they can also function as colorimetric/fluorometric sensors that produce naked-eye detectable sensing responses.

Gold nanoparticles (AuNPs) of 13 nm diameter are excellent colorimetric probes because of their unique localized surface plasmon resonance (LSPR) optical properties (Elghanian et al., 1997; Liu and Lu, 2004; Lim and Joo, 2006). A solution of well-dispersed AuNPs is red in color, while that of aggregated AuNPs is blue. Additionally, the extinction coefficient of AuNPs is high (3–5 orders of magnitude higher than that of organic chromophores) (Lee et al., 2007; Liu and Lu, 2004). These make 13 nm AuNPs sensitive signal transducers for chemo- and biosensing applications. Many researchers have proposed elegant ways to harness the LSPR responses of AuNPs with aptamers or DNAzymes/RNAzymes. However, modification of AuNPs with thiolated DNAzyme is an expensive and time-consuming process. Li and Rothberg have reported an effective strategy that made use of unmodified AuNPs for the rapid detection of DNA (Li and Rothberg, 2004a,b). Unmodified AuNPs can distinguish single-stranded DNAs (ssDNA) from double-stranded DNAs (dsDNA). Single-stranded DNAs can adsorb onto AuNPs and protect them from aggregation in a high ionic strength media, while dsDNAs cannot do so because of the

* Corresponding authors. Tel.: +86 551 63600843; fax: +86 551 63601592.
E-mail addresses: pstwmz@ustc.edu.cn (M. Wang), xwge@ustc.edu.cn (X. Ge).

0956-5663/$ - see front matter © 2013 Elsevier B.V. All rights reserved.
http://dx.doi.org/10.1016/j.bios.2013.10.016

electrostatic repulsion between their phosphate skeletons and the negatively charged AuNPs. To investigate the interactions between ssDNAs and AuNPs, Rothberg's group (Nelson and Rothberg, 2011) and Liu's group (Zhang et al., 2012; Liu, 2012) have conducted detailed works on the adsorption kinetics, capacity, isotherms and dominant forces in recent years. Due to its low cost and convenient operation, this signal transduction strategy has been extensively applied in biosensing, e.g. detection of lead ions (Wang et al., 2008b; Wei et al., 2008), mercury ions (Li et al., 2008, 2009a; Liu et al., 2008; Wang et al., 2008a; Xu et al., 2009), and ATP (Wang et al., 2007).

In these DNA-AuNP-based colorimetric sensors, signals are produced through conformational changes in the ssDNAs. Some guanine-rich ssDNA sequences can exhibit a conformational change from random coils to G-quadruplex structures in the presence of metal ions, such as K^+, Na^+, NH_4^+, and Pb^{2+} (Hardin et al., 2000; Shim et al., 2009). Pb^{2+} and K^+ are the most common ions that can stabilize G-quadruplexes, with Pb^{2+} being more effective than K^+ (Kotch et al., 2000; Smirnov and Shafer, 2000; Liu et al., 2012). G-quadruplex structures of DNAs play an important role in the regulation of cellular functions. They exist in telomeric DNAs and can inhibit telomerase activity (Gilbert and Feigon, 1999; Huang et al., 2007). Due to their high surface negative charge density, G-quadruplexes cannot adsorb onto AuNPs to protect them from aggregation (Huang et al., 2007; Wang et al., 2006). In this way, AuNPs can effectively differentiate between G-quadruplexes and random coiled ssDNAs. Based on this principle, Wang et al. (2006) reported a biosensor for K^+ ions. Obviously, the feasibility of this biosensing approach depends on the stability of G-quadruplexes in the presence of AuNPs. However, there have been reports about conformational changes to the secondary structures of DNAs upon their interaction with AuNPs. For example, Yang et al. (2007) have reported the dissociation of double-stranded DNAs (dsDNAs) by 5 nm AuNPs. In the biosensor field, 13 nm AuNPs are the most widely used signal transducers. Although the adsorption behavior of ssDNA onto 13 nm AuNP has been investigated (Nelson and Rothberg, 2011; Zhang et al., 2012; Liu, 2012), there was no report on the interaction between the secondary structures and AuNPs. In this work, three widely studied sequences: TBA, PW17, and PSO in the presence of Pb^{2+} and K^+ were used to study the interaction between G-quadruplexes and AuNPs, and we found that the stability of nanoparticles was enhanced in the G-quadruplex solutions, which is contrary to our general belief. The study of such interaction is of great significance because it may affect the sensitivity of these sensing systems.

2. Experimental

2.1. Materials and apparatus

All oligonucleotides (HPLC grade) were purchased from Sangon Biotechnology Inc. (Shanghai, China). The base sequences were as follows: TBA (5′-GGTTGGTGTGGTTGG-3′), PW17 (5′-GGGTAGGGC GGGTTGGG-3′), PSO (5′-GGGTTAGGGTTAGGGTTAGGG-3′), Mer18 (5′-CCAACCCCCCAGAAAGAA-3′), Mer16 (5′-CCAACCCCCAGAAGAA-3′) and C15 (5′-TAATAAAACAGGCCC-3′). DNA stock solutions were prepared by dissolving oligonucleotides in 14 mM Tris–HCl buffer (pH 7.4) (for TBA, PW17 and C15) or water (for PSO, Mer16 and Mer18), respectively. They were all heated to 94 °C to dissociate any intermolecular interaction followed by quenching in a 0 °C water bath. These oligonucleotide solutions were stored at 4 °C before use within one week. Their concentrations were determined by measuring their UV absorbance at 260 nm. The extinction coefficient (ε) for each nucleotide was: ε (dA)=15,400 M^{-1} cm^{-1}, ε (dG)=11,500 M^{-1} cm^{-1}, ε (dC)=7400 M^{-1} cm^{-1}, and ε (dT)=8700 M^{-1} cm^{-1}. Working solutions of TBA and PW17 were diluted with Tris–HCl buffer (pH 7.4, 14 mM) and that of PSO was diluted with water.

Gold nanoparticles of ca. 13 nm in diameter were synthesized using the citrate reduction method (Li et al., 2008; Liu and Lu, 2006) (see Supplementary materials). Acrylamide and *bis*-acrylamide (ultra pure grade) were purchased from Sangon Biotechnology Inc. (Shanghai, China). Ammonium persulfate and *N*, *N*, *N*′, *N*′-tetramethylethylenediamine were purchased from Bio-Rad. Standard solution of lead ion (Pb^{2+}) (1000 ppm, National Institute of Metrology, Beijing PR China) was diluted by water into a series of fresh working solutions of Pb^{2+} for use. All the other reagents (analytical reagent) were purchased from Sinopharm Chemical Reagent Co., Ltd (Shanghai, China), and were used as received. Milli-Q ultrapure water (18.2 MΩ cm) (Millpore Co., USA) was used throughout the study.

UV–vis absorption spectra were recorded using a Shimadzu UV-1800 UV–vis spectrophotometer equipped with a circular water bath to keep temperature constant. Photographs of polyacrylamide gels were taken with a Hewlett Packard (HP) scanjet 8200 scanner. All circular dichroism (CD) experiments were performed using a Jasco J-810 CD spectropolarimeter at 25 °C, maintained by a Julabo temperature controller. Conventional determinations of lead were conducted on a PerkinElmer 2100DV inductively coupled plasma atomic emission spectrometer (ICP-AES).

2.2. Adsorption kinetics of random coiled ssDNAs and G-quadruplexes onto AuNPs

2.2.1. Study of G-quadruplexes formed by Pb^{2+} and TBA or PW17

Working solution of TBA or PW17 (2.52 mL, 225 nM) was mixed with 700 μL of water (in the absence of Pb^{2+}) or Pb^{2+} solution at 20 °C for 2 h. Then, 3.080 mL of AuNPs solution (10 nM) was added. At predetermined intervals, 450 μL of this mixture was sampled and mixed with 50 μL of 250 mM NaCl solution. Absorbances of the resultant solution were measured at 520 nm and 650 nm after 3 min. The standard curves for the LSPR responses of the AuNPs (A_{650}/A_{520}) vs. pure ssDNA/AuNP ratio were prepared by mixing various concentrations of ssDNA with AuNPs and incubating for 5 h (for TBA) or 6 h (for PW17). To obtain the adsorption kinetics, the DNA/AuNP ratios at different incubation time were estimated through the A_{650}/A_{520} – DNA/AuNP ratio standard curves. By comparing with the total feeding amount of DNAs in the systems, the percentages of DNAs adsorbed on AuNPs were obtained.

2.2.2. Study of G-quadruplexes formed by K^+ and PSO

The PSO working solution (240 μL, 3.6 μM) and water (in the absence of K^+) or 200 mM of aqueous K^+ solution (12 μL) were mixed together at 20 °C for 2 h. Then 4.08 mL of Tris–HCl buffer (pH 7.4, 14 mM) was added, followed by 5.28 mL of AuNPs solution (10 nM). At predetermined intervals, 450 μL of this mixture was sampled and mixed with 50 μL of 275 mM NaCl solution. Absorbances of the resultant solution were measured at 520 nm and 650 nm after 3 min. The standard curve for the LSPR response of the AuNPs (A_{650}/A_{520}) vs. pure PSO/AuNP ratio was prepared by mixing various concentrations of pure PSO with AuNPs and incubating for 7 h.

2.3. Preparation of samples for ICP-AES

Working solution of DNA (TBA, PW17 and C15) (2.52 mL, 225 nM) was mixed with 700 μL of water (in the absence of Pb^{2+}) or Pb^{2+} solution (810 nM) at 20 °C for 2 h. Then, 3.080 mL of AuNPs solution (10 nM) was added. After 5 h (for TBA and C15)

or 6 h (for PW17) incubation, the solution was centrifuged at 15,000 rpm for 15 min. The supernatant solution was concentrated 4.5-fold through freeze drying and then the lead concentration was analyzed on an ICP-AES.

3. Results and discussion

3.1. The principle of the label-free ssDNA-unmodified AuNPs sensing system

AuNP of 13 nm diameter is an excellent colorimetric probe because of its characteristic surface plasmon resonance absorption band at 520 nm (See Fig. S1 and S2 in the Supplementary materials). AuNPs synthesized using the citrate reduction method are negatively charged, and have good dispersibility in water. The aqueous solution of AuNPs is red in colour (See Fig. S2). At high media ionic strength, the electrostatic repulsion between AuNPs will be screened, resulting in their aggregation. The solution becomes blue in color, with a shoulder absorption band developed at 650 nm (Fig. S2). The ratio of absorbance at 650 and 520 nm (A_{650}/A_{520}) is commonly used to reflect the degree of aggregation of AuNPs. It was reported that the random coiled ssDNAs in the aqueous solutions of AuNPs can protect the AuNPs from aggregation even at relatively high media ionic strength (See Fig. S2), as they can adsorb onto the AuNPs. However, dsDNAs or DNA strands with some other secondary structures, such as G-quadruplex structures, cannot adsorb onto AuNPs. They cannot stabilize the AuNPs against aggregation at high media ionic strength (Li and Rothberg, 2004b; Wang et al., 2006). This implies that unmodified AuNPs can be used to detect specific DNA or G-quadruplex structures. This phenomenon can also be exploited to detect metal ions, such as Pb^{2+}, as the formation of G-quadruplexes from guanine-rich ssDNAs depends on the presence of Pb^{2+}. Obviously, the reliability of such a sensing mechanism is built upon the assumption of no interference occurring between G-quadruplexes and AuNPs. However, Yang et al. (2007) have discovered that AuNPs with a diameter of 5 nm can dissociate double-stranded DNAs. Therefore, whether G-quadruplexes can be unfolded by 13 nm AuNPs has to be clarified before this sensing scheme can be effectively put into application.

3.2. The study on the interaction between G-quadruplexes and AuNPs

The formation of G-quadruplexes in these systems has been confirmed by their CD spectra (Fig. S3 in Supplementary materials). tbA is a thrombin-binding aptamer, which has been proved capable of forming G-Pb^{2+} (Smirnov and Shafer, 2000), and has been utilized to construct biosensors for Pb^{2+} (Liu et al., 2009). In general, 1 equiv of Pb^{2+} is enough to hold its G-quadruplex stable (Smirnov and Shafer, 2000; Li et al., 2009b). In our work, the molar ratio of TBA and Pb^{2+} adopted was 1:1.1. Under this condition, almost all of the TBA should be in the G-quadruplex conformation. If the G-quadruplex cannot be unfolded by AuNPs, the LSPR properties of the AuNP solution should remain unchanged. Fig. 1A shows the variation of the A_{650}/A_{520} ratio with time in pure TBA solution (Fig. 1A, black squares) and its Pb^{2+} stabilized G-quadruplex solution (TBA-Pb^{2+}) (Fig. 1A, red dots). The adsorption rate was fast at the beginning, reflected by the rapid decrease of A_{650}/A_{520} in the initial 10 min, and leveled off after about 100 min. Surprisingly, the TBA-Pb^{2+} solution displayed a similar LSPR as that of pure TBA solution. This implies that the G-quadruplex of TBA can also protect the AuNPs from aggregation. This observation is contrary to the general belief that the formation of G-quadruplexes would disfavor the adsorption of DNA strands onto AuNPs (Wang et al., 2005, 2006). Inspired by the report that 5 nm AuNPs can dissociate double-stranded DNA (Yang et al., 2007), we consider the possibility that G-quadruplexes may also be unfolded into random coiled ssDNA via strong interactions with gold nanoparticles. Fig. 1A (inset) shows that the LSPR response of the TBA-Pb^{2+} solution declined slower than that of the pure TBA solution. This indicates that the potential unfolding of the G-quadruplexes was coupled with the adsorption of the resultant ssDNAs onto AuNPs, and the concentration of the random coiled ssDNAs in the TBA-Pb^{2+} solution throughout the course was less than that in the pure TBA solution. This resulted in a slower adsorption rate of G-quadruplexes onto AuNPs. We have designed another assay to validate our hypothesis. We firstly mixed AuNPs with TBA and incubated for 5 h at room temperature, before the addition of Pb^{2+}. This was followed by the addition of NaCl solution at predetermined intervals. The LSPR properties of the AuNPs did not change with time, as displayed in Fig. 1A (green triangles). This indicates that the amount of ssDNAs adsorbed on AuNPs did not change after the addition of Pb^{2+}. What is more, the final value of A_{650}/A_{520} ratio was quite similar to that of pure TBA solution (at 5 h). These results further verify that the interaction between the ssDNAs and gold nanoparticles is much stronger than that between the ssDNAs and Pb^{2+}. This may be the driving force behind the unfolding of G-quadruplex by AuNPs.

In order to determine the degree of adsorption of DNAs in G-quadruplex solution, we plot a standard curve for the LSPR responses of the AuNPs (A_{650}/A_{520}) vs. pure TBA concentration (Fig. 1B). The standard curves were prepared under the same conditions to the analyzed DNA-AuNPs and G-quadruplex-AuNPs solutions, including the incubation time, salt concentration and aggregation time. The only difference is the presence of Pb^{2+} in the G-quadruplex solution. Thus, control experiments were performed to test the effect of Pb^{2+} on the aggregation behavior of AuNPs (see Supplementary materials). A series of solutions containing various [Pb^{2+}] (0-200 nM) were incubated for the same time as that in the preparation of the standard curve. The final concentration of Pb^{2+} before adding salt in the G-quadruplex-AuNPs solution is 110 nM. It can be seen from Fig. S5A that the AuNPs do not show aggregation in the Pb^{2+} concentration range we tested, which means the standard curve can be used to calibrate for the amount of DNA adsorbed on AuNPs, as shown in Table S1. In pure TBA solutions, up to 95% of the TBA ssDNA are adsorbed onto the AuNPs. In the TBA-Pb^{2+} system, our estimation showed that the AuNPs were able to adsorb most of the DNAs in G-quadruplex solution.

However, the G-quadruplex structures have some loops which are not arranged in the G-quartets and may be exposed to AuNPs. What is more, the buffer conditions in our work are different with that in Li and Rothberg's system. Therefore, we cannot conclude that the G-quadruplexes were unfolded by AuNPs. Another possibility which can induce these results is that the affinity of AuNPs for G-quadruplexes and ssDNAs is similar. Thus, two possibilities can be proposed to interpret the results observed. The first possibility is that G-quadruplexes can be adsorbed onto AuNPs and enhance the stability of these nanoparticles. The second possibility is that the G-quadruplexes are unfolded by AuNPs and it is the ssDNAs that protect the AuNPs. To investigate the dominant factor that causes these results, we designed an indirect strategy which used ICP-AES to analyze the lead concentration in the system. As is shown in Fig. 2A, after incubation, the Pb^{2+} ions exist on the surface of AuNPs in Possibility 1, while they exist in the solution in Possibility 2. These samples were centrifuged and the supernatant solutions were analyzed by ICP-AES. Here, a random ssDNA C15 which contains 15 bases was selected as the control sequence. This sequence has been analyzed by the Mfold

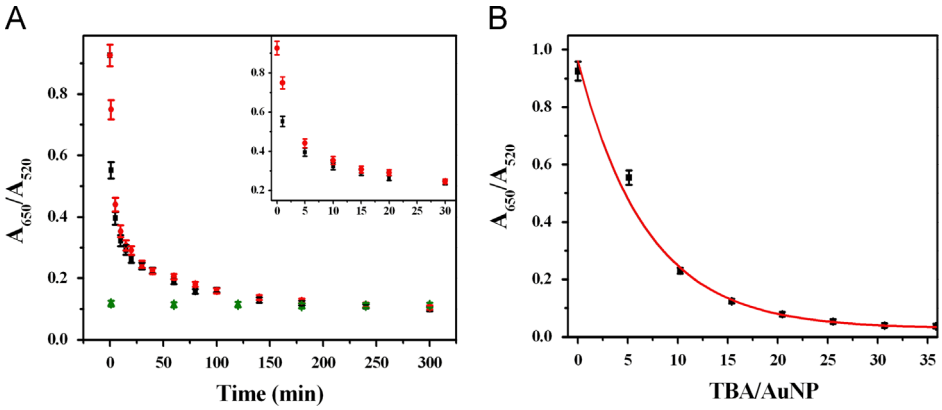

Fig. 1. (A) A_{650}/A_{520} vs. time curve of AuNPs solutions mixed with pure TBA solution (black squares) and TBA-Pb^{2+} (red dots). The relative standard deviation (RSD) was determined to be 3.8% and 3.6% in pure TBA and TBA-Pb^{2+} solutions, respectively (t=10 min, n=5). A_{650}/A_{520} vs. time curve of AuNPs-TBA solution mixed with Pb^{2+} (1 μM) (green triangles) (RSD=6.2% at t=10 min, n=5). AuNPs-TBA solution was prepared by 5 h adsorption of TBA onto AuNPs. The inset is the enlarged part from 0 to 30 min. (B) A_{650}/A_{520} vs. TBA/AuNP ratio curve of AuNPs in pure TBA solutions (RSD=4.4% at TBA/AuNP=10, n=5). The initial concentrations of TBA and AuNPs were 225 nM and 10 nM respectively. (For interpretation of the references to color in this figure legend, the reader is referred to the web version of this article.)

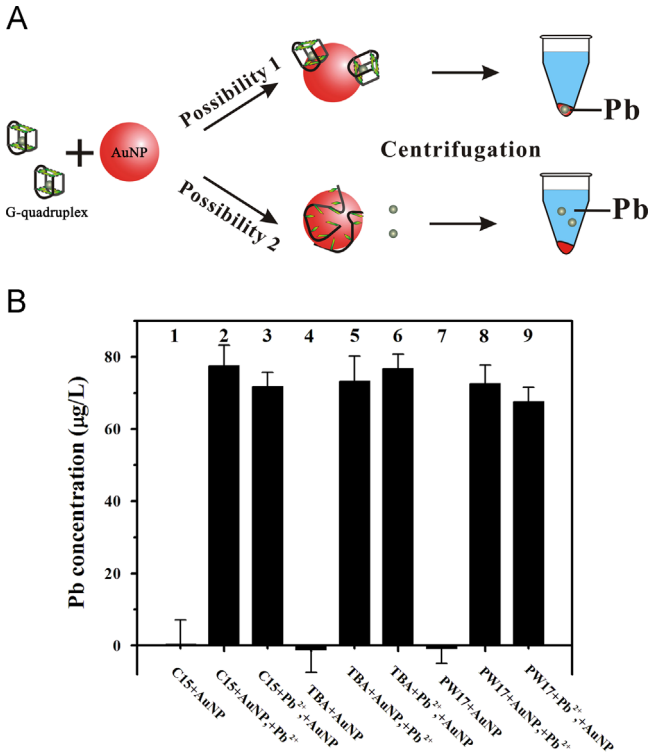

Fig. 2. (A) Schematic illustration of two possible adsorption styles. (B) Lead concentrations in the supernatant solutions of different samples analyzed by ICP-AES. DNA+AuNP represents that the ssDNA was adsorbed onto AuNP for 5 h (TBA and C15) or 6 h (PW17) (1, 4 and 7). DNA+AuNP, +Pb^{2+} represents that the ssDNA was adsorbed onto AuNP and then incubated with Pb^{2+} for 5 h (TBA and C15) or 6 h (PW17) (2, 5 and 8). DNA+Pb^{2+},+AuNP represents that the ssDNA was incubated with Pb^{2+} for 2 h, and then adsorbed onto AuNP for 5 h (TBA and C15) or 6 h(PW17) (3, 6 and 9).

(Zuker, 2003) and QGRS Mapper (Kikin et al., 2006) and results showed that there was no stable folded structure or G-quadruplex structure. The CD spectra also demonstrate that Pb^{2+} cannot induce conformation switch of C15 (Fig. S4 in the Supplementary materials). The limit of detection of ICP-AES for Pb has been determined to be 16.5 μg/L. To enhance the data reliability of the results, the supernatant solutions were concentrated 4.5-fold through freeze drying before ICP-AES measurements. According to the feeding amount of Pb^{2+}, we can estimate that the Pb concentration after freeze drying should be 405 nM (83.9 μg/L). From the ICP results (Fig. 2B), we can see that the Pb concentrations in all samples are lower than 83.9 μg/L, even in the system of control sequence C15. This difference may be attributed to the electrostatic interaction between negatively charged DNA strands or AuNPs and positively charged Pb^{2+}. In this work, the molar ratio of ssDNA and Pb^{2+} adopted was 1:1. Under this condition, most Pb^{2+} should be captured by ssDNA in TBA-Pb^{2+} systems, while it should be in a free state in C15-Pb^{2+} system. If the G-quadruplexes can be adsorbed onto AuNPs and still keep the conformation, the Pb concentrations in the TBA-Pb^{2+} system should be much lower than that in the C15-Pb^{2+} system after centrifugation. Fig. 2B shows the results of ICP measurements which were obtained by three independent experiments and the detailed data including the relative standard deviation (RSD) are shown in Table S4 (Supplementary materials). The results are contrary to this hypothesis because there is little difference in Pb concentrations between G-quadruplex system and control system (Fig. 2B, 3 and 5), and they are all much higher than ssDNA-AuNPs systems which do not contain Pb (Fig. 2B, 1 and 4). From Fig. 2B, 2 and 5, we can also see that the adsorbed TBA has no obvious interaction with Pb^{2+}. Therefore, we infer that the G-quadruplexes may be unfolded in the presence of AuNPs, releasing Pb^{2+} to water. This result may be caused by the strong affinity between DNA bases and AuNPs.

As for the PW17-Pb^{2+} system, it is more stable because of its more compact antiparallel structure. Fig. 3A shows the adsorption kinetics of random coiled PW17 (Fig. 3A, black squares) and the corresponding PW17-Pb^{2+} (Fig. 3A, red dots and green regular triangles) onto AuNPs. The PW17-Pb^{2+} G-quadruplexes may also be unfolded by AuNPs. The standard curve of A_{650}/A_{520} vs. PW17 concentration for pure PW17 solutions is shown in Fig. 3B. Compared with Fig. 1, the adsorption kinetics seems quite similar to that of the TBA-Pb^{2+} system. Through ICP analysis (Fig. 2B), the Pb concentration in the PW17-Pb^{2+} system is also similar to the control system (Fig. 2B, 3 and 9), and they are all much higher than the systems which do not contain Pb (Fig. 2B, 1 and 7). From Fig. 2B, 2 and 8, we can also see that the adsorbed PW17 has no obvious interaction with Pb^{2+}. Using the standard curves for the LSPR responses of the AuNPs (A_{650}/A_{520}) vs. pure DNA/AuNP ratio (Figs. 1B and 3B), it is easy to estimate the amount of adsorbed DNAs on the surface of AuNPs at different incubation time. Here we plotted the adsorption kinetics of DNAs in G-quadruplex solutions formed from TBA-Pb^{2+} and PW17-Pb^{2+}. Comparing the adsorption kinetics (Fig. 4) of these two systems, it is clearly seen that both the adsorption rate and the degree of adsorption of TBA-Pb^{2+} was larger than that of PW17-Pb^{2+}. The estimated

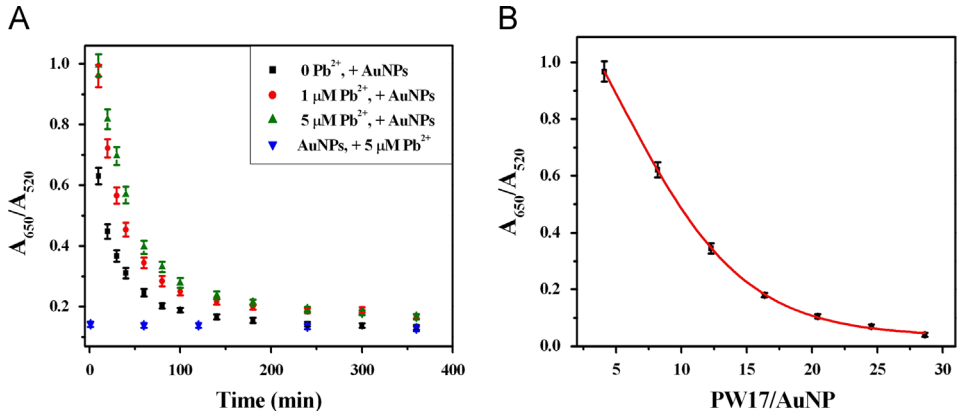

Fig. 3. (A) A_{650}/A_{520} vs. time curve of AuNPs solutions mixed with pure PW17 solution (black squares) and TBA-Pb^{2+} (red dots: 1 μM Pb^{2+}, green regular triangles: 5 μM Pb^{2+}). The RSD was determined to be 4.3%, 3.7% and 3.7% for the above three data, respectively (t=10 min, n=5). A_{650}/A_{520} vs. time curve of AuNPs-PW17 solution mixed with Pb^{2+} (5 μM) (blue inverted triangles) (RSD=6.0% at t=10 min, n=5). AuNPs-PW17 solution was prepared by 6 h adsorption of PW17 onto AuNPs. (B) A_{650}/A_{520} vs. PW17/AuNP ratio curve of AuNPs in pure PW17 solutions (RSD=4.2% at PW17/AuNP=10, n=5). The initial concentrations of TBA and AuNPs were 225 nM and 10 nM respectively. (For interpretation of the references to color in this figure legend, the reader is referred to the web version of this article.)

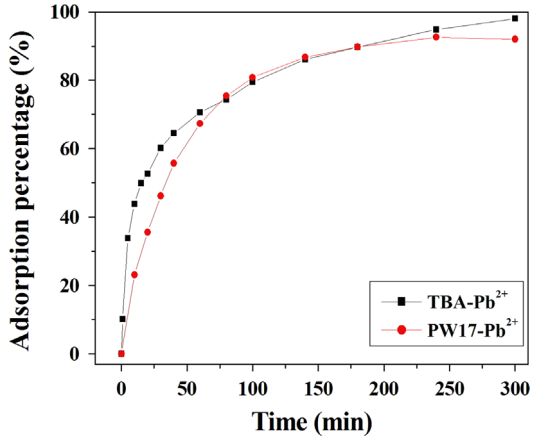

Fig. 4. Adsorption kinetics of DNAs in G-quadruplex solutions (TBA-Pb^{2+} and PW17-Pb^{2+}) in the presence of AuNPs.

percentage of ssDNA adsorbed onto AuNPs of the two systems was measured and tabulated in Table S2 (Supplementary materials). Their differences in the adsorption behaviors may be caused by their different molecular structures and composition. TBA is a shorter DNA strand and the intramolecular tension of its G-quadruplex conformation must be higher than that of the longer strand PW17. What is more, PW17 possesses 12 guanines that can interact with Pb^{2+}, while TBA only has 9. All these factors make PW17-Pb^{2+} more stable in the presence of AuNPs.

Summarizing our results, the interaction between 13 nm AuNPs and ssDNAs is much stronger than that between Pb^{2+} and ssDNAs, and may result in the unfolding of the Pb^{2+}-stabilized G-quadruplexes.

Recently, studies on the application of K^+ stabilized G-quadruplex (G-K^+) in colorimetric sensors have been reported by Wang et al. (2006). Here, we also investigated the adsorption behavior of PSO in G-quadruplex solution formed by PSO and K^+ (PSO-K^+). Fig. 5A shows the adsorption kinetics of random coiled PSO (Fig. 5A, black squares) and PSO-K^+ (Fig. 5A, red dots) onto AuNPs. The standard curve of the LSPR response of AuNPs (A_{650}/A_{520}) vs. pure PSO concentration is shown in Fig. 5B. The standard curve is prepared similar to that in the TBA and PW17 systems. The K^+ ions used in this studied (final concentration is 0.25 mM) do not produce obvious aggregation of AuNPs (See Fig. S5B in the Supplementary materials). It is well known that K^+ has a lower efficiency in stabilizing G-quadruplexes in comparison with Pb^{2+} (Li et al., 2009b). This implies that PSO-K^+ can be more easily unfolded by AuNPs. The adsorption kinetics of PSO-K^+ displayed in Fig. 5A is similar to that of the TBA-Pb^{2+} and PW17-Pb^{2+} systems. However, the degree of adsorption in the PSO-K^+ system is more complicated because the K^+/ssDNAs ratio in the corresponding G-quadruplex solution is not clear. To obtain the percentage of random coiled PSO or PSO-K^+ in the presence of a certain concentration of K^+, we conducted non-denaturing polyacrylamide gel electrophoresis to separate ssDNAs with different configuration. From the PAGE results (Fig S6 in Supplementary materials), it is estimated that 67 ± 4% of the PSO formed G-quadruplexes in the presence of 10 mM K^+. If AuNPs cannot adsorb the PSO-K^+ G-quadruplexes, only about 33% of the PSO would be adsorbed onto AuNPs. In fact, the LSPR response of the AuNPs in the PSO-K^+ system (Fig. 5A, red dots) corresponds to 77% of PSO adsorbed on AuNPs (Table S3 in Supplementary materials). This result has unambiguously showed that more PSO from G-quadruplexes have been adsorbed onto AuNPs.

3.3. *The detection of Pb^{2+} ions using PW17 as the sensing unit*

Although the potential unfolding of G-quadruplexes by AuNPs renders ssDNA – Aed if an appropriate incubation tiuNPs biosensors less sensitive, analyte detection can still be performme of DNA and AuNPs can be selected to alleviate such impact. A sensing system consisting of PW17 and AuNPs was developed to detect the concentration of Pb^{2+}. The LSPR responses of the sensing system are sensitive to [Pb^{2+}] (Fig. S7 in Supplementary materials). According to the above results, we know that PW17-Pb^{2+} is comparatively stable. Both its adsorption rate and the degree of G-quadruplex adsorption are much lower than those of the TBA-Pb^{2+}. Therefore, we attempted to design a biosensor for the detection of Pb^{2+} based on label-free PW17 and unmodified AuNPs. It can be seen from the adsorption behavior of PW17 and its G-quadruplexes onto AuNPs (Fig. 3A) that the incubation time of DNAs and AuNPs has an important influence on sensibility. The difference between A_{650}/A_{520} for random coiled PW17 and that for its G-quadruplexes decreased with time. At the beginning, the difference was 0.4 when 1 μM Pb^{2+} was added and it decreased to 0.143 after 40 min and 0.035 after 6 h. We can conclude that long time incubation makes it unable to distinguish random coiled and G-quadruplex DNAs. Thus, less incubation time is suggested to make the system more sensitive. However, large data variance may be measured during the first several minutes due to high adsorption rate and it is hard to obtain an accurate calibration curve

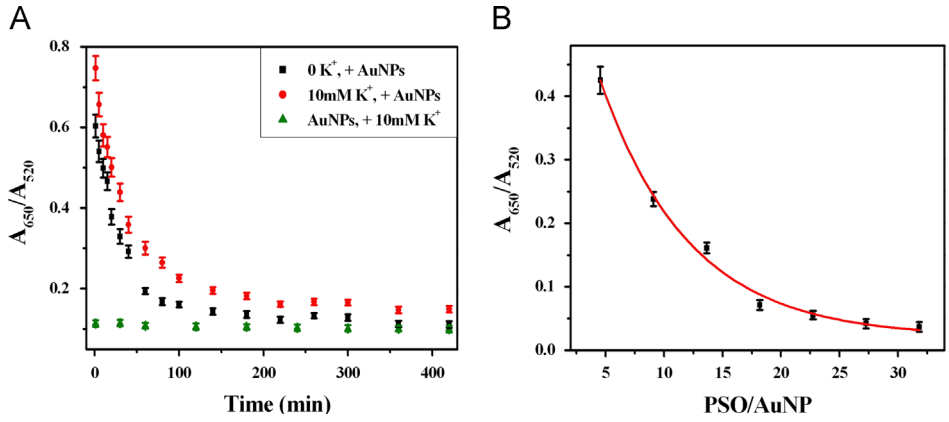

Fig. 5. (A) A_{650}/A_{520} vs. time curve of AuNPs solutions mixed with pure PSO solution (black squares) and PSO-K^+ (red circles). RSD was determined to be 4.6% and 4.1% for the above two data, respectively (t=10 min, n=5). A_{650}/A_{520} vs. time curve of AuNPs-PSO solution mixed with K^+ (green triangles) (RSD=6.2% at t=10 min). AuNPs-PSO solution was prepared by 7 h adsorption of PSO onto AuNPs. (B) A_{650}/A_{520} vs. PSO/AuNP ratio curve of AuNPs in pure PSO solutions (RSD=4.7% at PSO/AuNP=10, n=5). (For interpretation of the references to color in this figure legend, the reader is referred to the web version of this article.)

without the assistance of special equipment. Therefore, 20 min′ adsorption time for PW17 and AuNPs was selected before the addition of salt solution. Fig. S7 shows the LSPR responses of the AuNPs (A_{650}/A_{520}) vs. Pb^{2+} concentration ([Pb^{2+}]) at different PW17 concentrations ([PW17]). Evidently, the LSPR response is sensitive to [Pb^{2+}]. However, the accuracy of the system deteriorated at a lower [PW17]. For example, when [PW17] was 50 nM (Fig. S7A), the sensing range was narrow (0–0.02 μM) and the variance in measured data was large. With the increasing of [PW17], the variance in measured data became smaller, and the sensing range was enlarged. When [PW17] was higher (200 nM, Fig. S7E), the effect of [PW17] on the sensing range became less significant. Compared to recent reported DNAzyme-based fluorescence biosensors for Pb^{2+} detection, which achieved a detection limit of 0.4 nM of [Pb^{2+}] and a detection range from 1 to 1000 nM (Kim et al., 2011; Li et al., 2011), our PW17-unmodified AuNPs sensing system is less sensitive. These results demonstrate the adverse effect of the potential unfolding of G-quadruplexes on the sensitivity of the sensing approach. Therefore, it is imperative that this phenomenon is being taken note of in the design of an aptamer-AuNP system and G-quadruplexes with higher stability against unfolding by AuNPs should be selected in the future development of this biosensing system.

4. Conclusion

In this work, the adsorption behavior of random coiled single-stranded DNAs (ssDNAs) and G-quadruplexes onto AuNPs in solutions of TBA-Pb^{2+}, PW17-Pb^{2+}, and PSO-K^+ respectively were studied through the LSPR responses of AuNPs (A_{650}/A_{520}). For Pb^{2+} stabilized G-quadruplexes (G-Pb^{2+}), the degree of adsorption was found to be as high as 93% when the adsorption time for ssDNAs and AuNPs was beyond 2 h. The lead concentrations in the G-quadruplexes – AuNPs solutions after the removal of AuNPs detected by ICP-AES was found to be similar to that in the control DNA-AuNPs system, demonstrating that the lead located in G-quadruplexes had been released. This implied that G-quadruplexes may be unfolded in the presence of AuNPs. However, the question on whether the G-quadruplexes are first adsorbed on AuNPs and then unfolded, or whether the G-quadruplexes are first unfolded in the driving of the interaction between G-quadruplexes and AuNPs, and then ssDNAs are adsorbed onto AuNPs, still needs further investigations. The potential unfolding of G-quadruplexes makes the sensitivity to [Pb^{2+}] of the sensing system consisting of PW17 and AuNPs debilitated. Therefore, the unexpected adverse effect of AuNPs on DNA-based biosensors we have found in this work should be taken into consideration in the future development of biosensing systems that are based on ssDNA aptamers and unmodified AuNPs.

Acknowledgments

The authors gratefully acknowledge the National Natural Science Foundation of China (Nos. 20934004, 51073146, 51103143, and 51173175), the Natural Basic Research Program of China (Nos. 2012CB821500 and 2010CB934500), the Fundamental Research Funds for the Central Universities (No. WK2060200005, 2010) and "Bairen" fund of CAS.

Appendix A. Supplementary material

Supplementary data associated with this article can be found in the online version at http://dx.doi.org/10.1016/j.bios.2013.10.016.

References

Breaker, R.R., 1997. Curr. Opin. Chem. Biol. 1 (1), 26–31.
Chavez, J.L., Lyon, W., Kelley-Loughnane, N., Stone, M.O., 2010. Biosens. Bioelectron. 26 (1), 23–28.
Elghanian, R., Storhoff, J.J., Mucic, R.C., Letsinger, R.L., Mirkin, C.A., 1997. Science 277 (5329), 1078–1081.
Ellington, A.D., Szostak, J.W., 1990. Nature 346, 818–822.
Gilbert, D.E., Feigon, J., 1999. Curr. Opin. Struc. Biol 9 (3), 305–314.
Hardin, C.C., Perry, A.G., White, K., 2000. Biopolymers 56 (3), 147–194.
Huang, C.Z., Liao, Q.G., Gan, L.H., Guo, F.L., Li, Y.F., 2007. Anal. Chim. Acta 604 (2), 165–169.
Jayasena, S.D., 1999. Clin. Chem. 45 (9), 1628–1650.
Kikin, O., D'Antonio, L., Bagga, P.S., 2006. Nucleic Acids Res. 34 (Suppl 2), W676–W682.
Kim, J.H., Han, S.H., Chung, B.H., 2011. Biosens. Bioelectron. 26 (5), 2125–2129.
Kotch, F.W., Fettinger, J.C., Davis, J.T., 2000. Org. Lett. 2 (21), 3277–3280.
Lee, J.S., Han, M.S., Mirkin, C.A., 2007. Angew. Chem. Int. Ed. 46 (22), 4093–4096.
Li, C.L., Liu, K.T., Lin, Y.W., Chang, H.T., 2011. Anal. Chem. 83 (1), 225–230.
Li, D., Wieckowska, A., Willner, I., 2008. Angew. Chem. Int. Ed. 47 (21), 3927–3931.
Li, H.X., Rothberg, L., 2004a. Proc. Natl. Acad. Sci. USA 101 (39), 14036–14039.
Li, H.X., Rothberg, L.J., 2004b. J. Am. Chem. Soc. 126 (35), 10958–10961.
Li, L., Li, B.X., Qi, Y.Y., Jin, Y., 2009a. Anal. Bioanal. Chem. 393 (8), 2051–2057.
Li, T., Dong, S.J., Wang, E.K., 2010a. J. Am. Chem. Soc. 132 (38), 13156–13157.
Li, T., Wang, E., Dong, S., 2010b. Anal. Chem. 82 (4), 1515–1520.
Li, T., Wang, E.K., Dong, S.J., 2009b. J. Am. Chem. Soc. 131 (42), 15082–15083.
Lim, J.K., Joo, S.-W., 2006. Appl. Spectrosc. 60 (8), 847–852.
Liu, C.W., Hsieh, Y.T., Huang, C.C., Lin, Z.H., Chang, H.T., 2008. Chem. Commun. 19, 2242–2244.
Liu, C.W., Huang, C.C., Chang, H.T., 2009. Anal. Chem. 81 (6), 2383–2387.
Liu, J., 2012. Phys. Chem. Chem. Phys. 14 (30), 10485–10496.
Liu, J., Lu, Y., 2006. Nat. Protoc. 1 (1), 246–252.
Liu, J.W., Lu, Y., 2003. J. Am. Chem. Soc. 125 (22), 6642–6643.

Liu, J.W., Lu, Y., 2004. J. Am. Chem. Soc. 126 (39), 12298–12305.
Liu, W., Zhu, H., Zheng, B., Cheng, S., Fu, Y., Li, W., Lau, T.-C., Liang, H., 2012. Nucleic Acids Res. 40 (9), 4229–4236.
Nelson, E.M., Rothberg, L.J., 2011. Langmuir 27 (5), 1770–1777.
Shim, J.W., Tan, Q.L., Gu, L.Q., 2009. Nucleic Acids Res. 37 (3), 972–982.
Smirnov, I., Shafer, R.H., 2000. J. Mol. Biol. 296 (1), 1–5.
Ueyama, H., Takagi, M., Takenaka, S., 2002. J. Am. Chem. Soc. 124 (48), 14286–14287.
Wang, H., Wang, Y.X., Jin, J.Y., Yang, R.H., 2008a. Anal. Chem. 80 (23), 9021–9028.
Wang, J., Wang, L.H., Liu, X.F., Liang, Z.Q., Song, S.P., Li, W.X., Li, G.X., Fan, C.H., 2007. Adv. Mater. 19 (22), 3943–3946.
Wang, L.H., Liu, X.F., Hu, X.F., Song, S.P., Fan, C.H., 2006. Chem. Commun. 36, 3780–3782.
Wang, S., He, F., Tang, Y.L., Li, Y.L., Zhu, D.B., 2005. J. Am. Chem. Soc. 127 (35), 12343–12346.
Wang, Z.D., Lee, J.H., Lu, Y., 2008b. Adv. Mater. 20 (17), 3263–3267.
Wei, H., Li, B.L., Li, J., Dong, S.J., Wang, E.K., 2008. Nanotechnology 19 (9), 095501.
Xu, X.W., Wang, J., Jiao, K., Yang, X.R., 2009. Biosens. Bioelectron. 24 (10), 3153–3158.
Yang, C., Wang, Y., Marty, J.L., Yang, X.R., 2011. Biosens. Bioelectron. 26 (5), 2724–2727.
Yang, J., Pong, B.K., Lee, J.Y., Too, H.P., 2007. J. Inorg. Biochem. 101 (5), 824–830.
Zhang, J., Chen, P.P., Wu, X.Y., Chen, J.H., Xu, L.J., Chen, G.N., Fu, F.F., 2011. Biosens. Bioelectron. 26 (5), 2645–2650.
Zhang, J., Wang, L.H., Pan, D., Song, S.P., Boey, F.Y.C., Zhang, H., Fan, C.H., 2008. Small 4 (8), 1196–1200.
Zhang, X., Servos, M.R., Liu, J., 2012. Langmuir 28 (8), 3896–3902.
Zuker, M., 2003. Nucleic Acids Res. 31 (13), 3406–3415.